THE ARCHIVE OF MECHANICAL ENGINEERING

Vol. XLVIII 2001 Number 1

Key words: *biaxial fatigue, variable amplitude, non-proportional loading, energy criterion, life time*

TADEUSZ LAGODA[*], *EWALD MACHA*[*], *ADAM NIESLONY*[*], *ANDREAS MÜLLER*[**]

FATIGUE LIFE OF CAST IRONS GGG40, GGG60 AND GTS45 UNDER COMBINED VARIABLE AMPLITUDE TENSION WITH TORSION

The paper contains the fatigue tests results for specimens made of three cast irons under proportional and non-proportional variable amplitude tension with torsion. The experimental data for long fatigue life have been compared with those calculated according to the algorithm with use of the modified criterion of the maximum normal stress in the critical plane. In the considered algorithm the Palmgren-Miner hypothesis of damage cumulation seems to be useless whereas the Serensen-Kogayev hypothesis gives satisfactory results. Applying the method of fatigue damage cumulation we obtain the critical plane direction which agrees with the experimental fracture plane very well.

Nomenclatures:

- a — coefficient including influence of amplitudes less then the fatigue limit,
- l_η, m_η — direction cosines,
- m — Wöhler curve exponent,
- N — number of cycles,
- r — correlation coefficient,
- S — damage degree,
- t — time,
- T_0 — observation time,

[*] *Technical University of Opole, Department of Mechanics and Machine Design, ul. Mikolajczyka 5, 45-271 Opole, Poland; E-mail: tlag@po.opole.pl, emac@po.opole.pl, nieslony@bet.po.opole.pl;*

[**] *Fraunhofer-Institut für Betriebsfestigkeit Darmstadt, now: BMW AG, EG-542, D-80788 München, Germany; E-mail: Andreas.MF.Mueller@bmw.de*

φ — angle between the longitudinal axis of the specimen and the direction of the critical plane,
σ — normal stress,
σ_{af} — fatigue limit for tension,
τ — shear stress,
τ_{af} — fatigue limit for torsion.

Indexes:
cal — calculated,
CD — Corten-Dolan hypothesis,
eq — equivalent,
exp — experimental,
PM — Palmgren-Miner,
SK — Serensen-Kogayev.

1. Introduction

The known algorithms of fatigue life estimation in elements of machines and structures under multiaxial random or variable amplitude loading are not well supported by the experimental results. The load with variable amplitudes, as a particular case of random loading, is often applied in fatigue tests. Wang and Brown [13], Fatemi and Socie [19] propose to use the shear and normal strain in the critical plane as a quantity influencing the fatigue process. Morel [14] suggest to apply the normal and shear stress in the critical plane for estimation of the fatigue life, similarly as Papadopoulosa [15]. Lately Łagoda at al. [1], Socie [12] Perov at al. [17] and Lease and Stephnens [16] try to use the parameter of strain energy density in the critical plane, similar to the SWT parameter [18]. Some of those algorithms have been verified for certain steels [1], [12], [13], [14], [15], [16], [17], but we do not know if they are also efficient in the case of cast irons. The aim of this paper is to verify the algorithm presented in paper [11] for three cast irons. The specimens were subjected to combined variable amplitude tension with torsion.

2. Fatigue tests

The fatigue tests were done on a stand for tension-compression with torsion, made by Schenck (series 31), in LBF laboratories in Darmstadt, Germany [2], [3], [4]. While the machine operating, the force was controlled. The specimens were made of three materials: spheroidal cast irons GGG40 and GGG60 and malleable cast iron GTS45. On the basis of microscopic examination, the materials could be classified as isotropic. The materials are cyclically hardened. The basic strength parameters are shown in Table 1. The details concerning the realized fatigue tests are given in [2], [3], [4]. Cylindrical specimens with solid

cores were used in the tests. The specimen dimensions are given in Fig. 1. The specimens of GGG40 and GTS45 and of GGG60 were different but they had the same minimal diameter at the bottom of the spherical relief and the notch effect coefficient for tension – compression α_k was 1.05 for specimen a) and 1.04 for specimen b). These differences do not strongly influence the results of experiments and they can be neglected. For further considerations we assume that the applied specimens have the same shape and the notch coefficient α_k is 1, so they are the smooth specimens.

Table 1.

Basic strength parameters of the tested cast irons

		GGG40	GGG60	GTS45
$R_{0.2}$	MPa	322	427	310
R_m	MPa	440	649	469
A_5	%	10.9	10.6	9.4
Z	%	10.6	9.7	8.1
E	GPa	167	160	167
ν	1	0.29	0.29	0.27

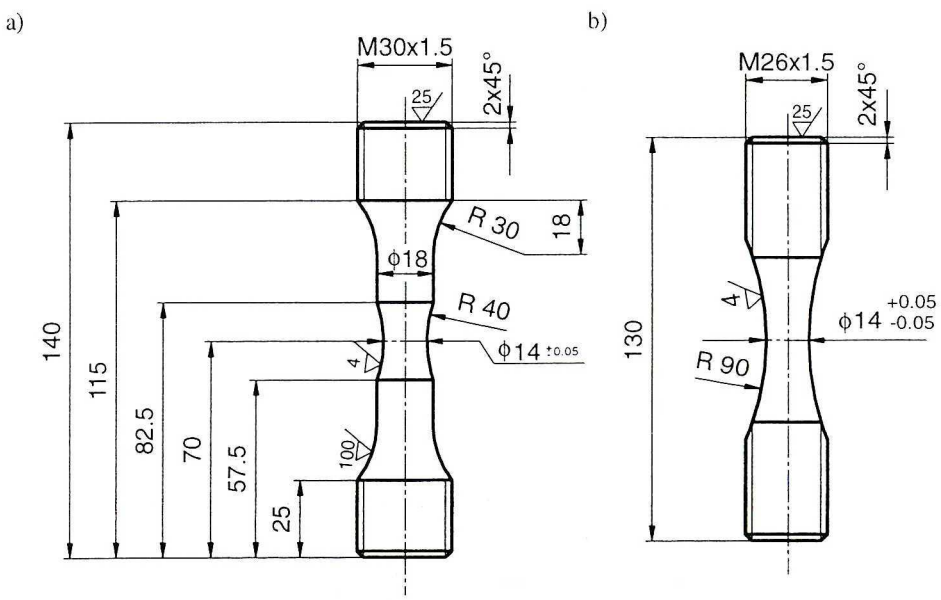

Fig. 1. Specimens used in tests a) cast irons GGG40 and GTS45, b) cast iron GGG60

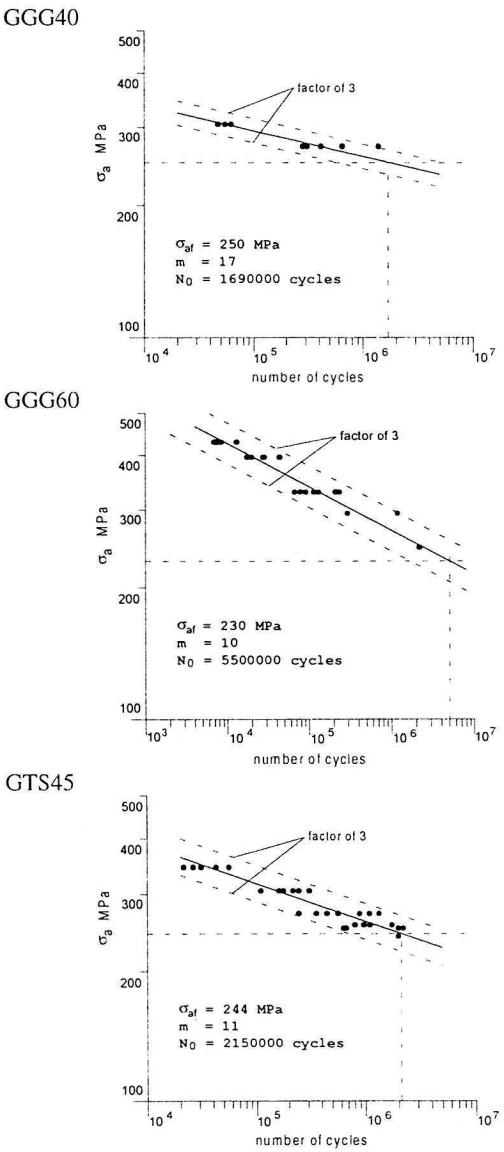

Fig.2 Experimental fatigue lives against the Wöhler curves for uniaxial tension-compression

Fig. 2 shows the experimental results for cyclic tension-compression against the Wöhler curve. From the figure it appears that the scatter of the experimental results for uniaxial cyclic tests is included into the scatter band of coefficient 3. Some results, however, are included into the scatter band of coefficient 4. Thus, if the calculated fatigue life for multiaxial variable amplitude and the experimental results are included into these scatter bands, we can say that such results are satisfactory.

In the case of uniaxial tension-compression and torsion, loading was applied with use of a digitally generated standard time series g(t) with zero expected value. The series was suitably scaled for obtaining the required maximum histories of normal stress, σ_{max} and shear stress, τ_{max}. In the case of combined tension-compression with torsion, we realized proportional loading with the correlation coefficient of normal and shear stress equal to 1 ($r_{\sigma,\tau} = 1$) and non-proportional loading with the stress correlation coefficient equal to 0 ($r_{\sigma,\tau} \approx 0$). The coefficient was determined from

$$r_{\sigma,\tau} = \frac{\mu_{\sigma\tau}}{\sqrt{\mu_\sigma \mu_\tau}} \tag{1}$$

Where: μ_σ, μ_τ, $\mu_{\sigma\tau}$ – components of the stress covariance matrix.

Uncorrelated stress histories were obtained with use of frequency modulation of loading generating normal stress under the standard history g(t) in torsional loading. For both proportional and non-proportional loading relation between the maximum values of tensile stress $\sigma_{xx\ max}$ and torsional stress $\tau_{xy\ max}$ was 1. Frequency of torsion history extrema was constant and frequency of tension-compression history extrema was changing (the normal stress increment between the successive extrema at time was constant).

Loading was applied according to the standard course, written in digits. That course contains a sequence of numbers of normal distribution, corresponding to successive extrema. Discrete values between the extrema are obtained by joining two following numbers with a curve being a half of cosinus. Under tension-compression frequency of the extrema was $f_\sigma = 10.4$ Hz and under torsion $f_\tau = 7.8$ Hz.

Under correlated biaxial loading the frequency of extrema was the same for tension-compression and torsion and it was $f_\sigma = f_\tau = 6$ Hz. The uncorrelated course was realized by frequency modulation of local extrema of normal loading. Under torsion the frequency of extrema was constant, $f_\tau = 6$ Hz. For tension-compression it changed in the range $3.0 \leq f_\sigma \leq 7.8$ Hz in such a way that the stress increment between the successive extrema at time was constant. Moreover, the beginning of the standard course for torsion was shifted by 30848 cycles in relation of the normal stress course. The expected value was 0, like in the case of the correlated loading. A frequency change under tension-compression introduces an irregularity to a genaral form of multiaxial fatigue.

Fatigue loading totally includes 126 results of the experiments obtained under variable amplitudes. Numbers of cycles up to fracture have large scatters. Thus, it is difficult to verify the proposed calculation models. For example, in the case of GGG40 cast iron under tension-compression and the maximum stress amplitude 300 MPa, the minimal life is $1.937 \cdot 10^6$ cycles and the maximum one $19 \cdot 10^6$ cycles, so tenfold scatter is observed. In the case of proportional loading with normal and shear stress correlation coefficient equal to 1 ($r_{\sigma,\tau} = 1$), we can observe a greater life than in the case of non-proportional loading with the stress correlation coefficient equal to 0 ($r_{\sigma,\tau} \approx 0$) for the same maximum stress levels.

3. Algorithm for fatigue life determination

Figure 3 shows a diagram of the algorithm for fatigue life determination under multiaxial random loading. The algorithm was used for the analysis of experimental data.

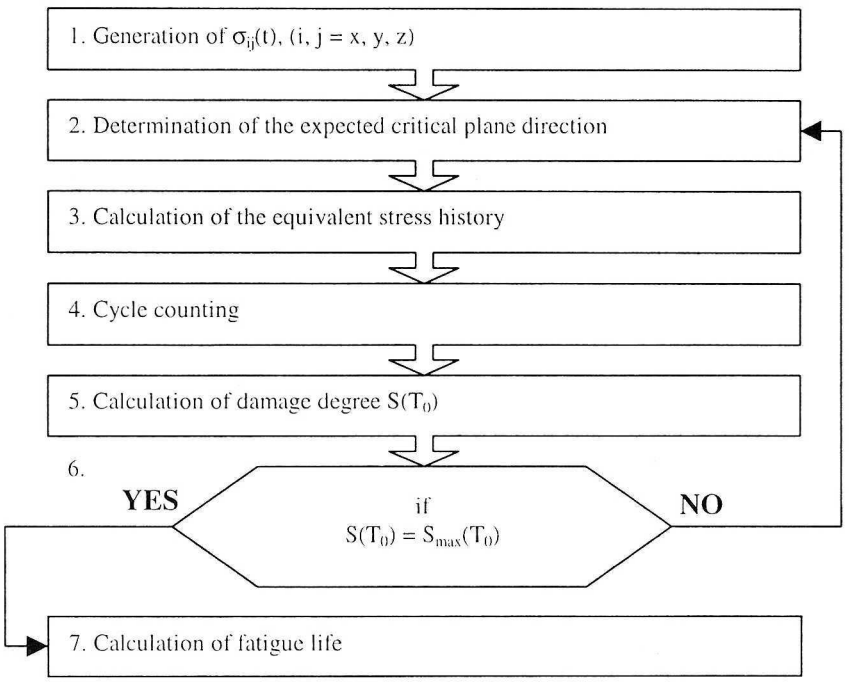

Fig. 3. Algorithm for fatigue life determination under multiaxial random loading

The stress $\sigma_{ij}(t)$ was generated in the same way as during experiments, by a suitable scaling of the standard history g(t). For determination of the expected direction of the critical plane, the damage cumulation method was applied. In this method, the fatigue damage is cumulated at many planes; next the plane of the maximum damage is chosen. In such a way, we obtain not only a direction of the expected fracture plane but the fatigue life as well [1].

For determination of the equivalent stress, the criterion of maximum normal stress in the fracture plane was applied. The criterion was modified, by the ratio of the fatigue limits for tension and torsion, i.e. [6]

$$\sigma_{eq}(t) = l_\eta^2 \cdot \sigma(t) + 2 l_\eta m_\eta \frac{\sigma_{af}}{\tau_{af}} \cdot \tau(t) \tag{2}$$

where:

$$l_\eta = \cos(\varphi), \tag{3}$$

$$m_\eta = \sin(\varphi), \tag{4}$$

φ - angle between the longitudinal axis of the specimen and the expected direction of the critical plane $\overline{\eta}(l_\eta, m_\eta)$,

$\sigma(t)$, $\tau(t)$ – histories of the normal and shear stress,

σ_{af}, τ_{af} – fatigue limits for tension and torsion, respectively.

In this paper, the rain flow method [5] was used for schematization of variable amplitude histories. This method allows us to separate cycles and half-cycles of stress, amplitudes and the mean value. The exemplary two-parameter probability density function of the equivalent course subjected to schematization is shown in Figs. 4 and 5 for two cases: loading by tension-compression (GGG40, $\sigma_{xx\ max}$ = 300 MPa, φ = 0 degrees) and non-correlated loading (GGG40, $\sigma_{xx\ max} = \tau_{xy\ max}$ = 255 MPa, φ = 33 degrees). From these figures it appears that participation of positive and negative mean values of cycles is the same and can be neglected.

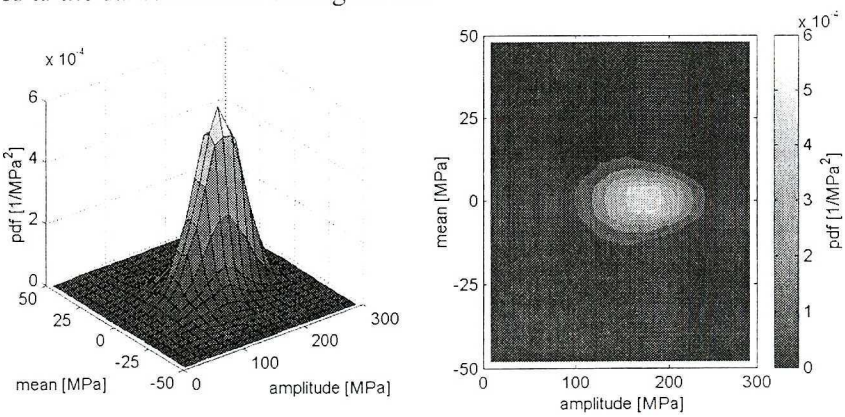

Fig. 4. Two-parameter probability density function (pdf) of load cycles (σ_{max}=300 MPa, uniaxial tension)

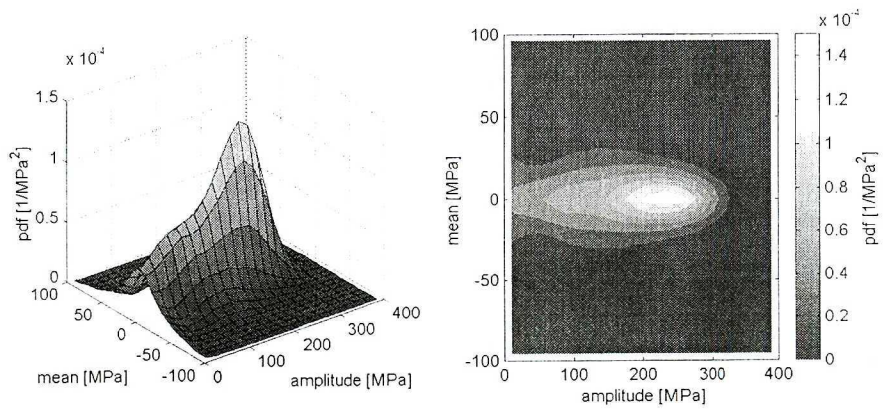

Fig. 5. Two-parameter probability density function (pdf) of load cycles (σ_{max}=τ_{max}=255 MPa, nonproportional tension with torsion)

For damage accumulation, three hypotheses were applied, i.e.:
Palmgren-Miner hypothesis [8], [9]

$$S_{PM}(T_0)=\begin{cases}\displaystyle\sum_{i=1}^{j}\frac{n_i}{N_0\left(\frac{\sigma_{af}}{\sigma_{ai}}\right)^m} & \text{for } \sigma_{ai}\geq a\cdot\sigma_{af}\\ 0 & \text{for } \sigma_{ai}<a\cdot\sigma_{af}\end{cases} \tag{5}$$

where:
n_i — number of cycles with amplitudes σ_{ai} in T_0,
m — Wöhler curve exponent,
N_0 — number of cycles corresponding to the fatigue limit σ_{af},
T_0 — observation time equal to 1 block including 50048 cycles,
$a = 0.5$ — coefficient including influence of amplitudes less than the limit σ_{af}.

Corten – Dolan hypothesis [7]

$$S_{CD}(T_0)=\sum_{i=1}^{j}\frac{n_i}{N_1}\left(\frac{\sigma_{ai}}{\sigma_{a1}}\right)^{qCD} \quad \text{for } \sigma_{ai}\leq\sigma_{a1} \tag{6}$$

where:
σ_{a1}, N_1 – maximum cycle amplitude at T_0 and corresponding number of cycles to fracture,
$q_{CD} = k\cdot m$ – exponent of the secondary calculation Wöhler's curve (Cortan – Dolan curve),
$k = 0.7 \div 1.0$ and it depends on σ_{ai}/σ_{af}.

Serensen-Kogayev hypothesis [10]

$$S_{SK}(T_0)=\begin{cases}\displaystyle\sum_{i=1}^{j}\frac{n_i}{b\ N_0\left(\frac{\sigma_{af}}{\sigma_{ai}}\right)^m} & \text{for } \sigma_{ai}\geq a\cdot\sigma_{af}\\ 0 & \text{for } \sigma_{ai}<a\cdot\sigma_{af}\end{cases} \tag{7}$$

where:

$$b=\frac{\displaystyle\sum_{i=1}^{k}\sigma_{ai}t_i-a\cdot\sigma_{af}}{\sigma_{a1}-a\cdot\sigma_{af}} \quad \text{for } (b>0.1) \text{ - Serensen-Kogayev coefficient,}$$

$$t_i=\frac{n_i}{\displaystyle\sum_{i=1}^{k}n_i} \text{ - frequency of occurence of particular levels } \sigma_{ai} \text{ in } T_0,$$

$a = 0.6$ for Serensen-Kogayev hypothesis.

When the damage degree $S(T_0)$ is determined at T_0 according to (5), (6) or (7), we calculate the fatigue life

$$N_{cal} = \frac{T_o}{S(T_o)}, \tag{8}$$

where N_{cal} = the calculated number of cycles to fracture.

4. Comparison of calculated and experimental lives

Figures 6, 7 and 8 shows comparison of calculated and experimental lives for uniaxial tension-compression according to three considered hypotheses of fatigue damage accumulation. Calculations of the fatigue life N_{cal} were done according the algorithm presented in Fig. 3 and with the use of relation (8). We can observe that the calculated lives are higher than those obtained while experiments when Palmgren-Miner and Corten-Dolan hypotheses are applied. It could be seen especially under uniaxial loading, where the maxima of the equivalent stress histories are close to the fatigue limit σ_{af}. Applying the Serensen-Kogayev hypothesis, we obtain the best agreement between the calculated and experimental lives. All the results obtained with use of that hypothesis are included in the scatter band with coefficient 3. Only for cast iron GTS45 we obtain greater scatters.

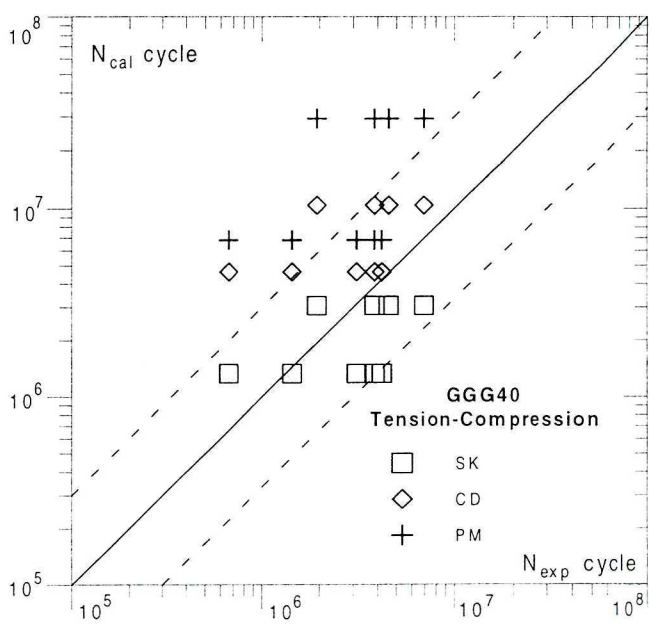

Fig. 6. Comparison of the calculated life N_{cal} and the experimental one N_{exp} for cast iron GGG40 under variable amplitude tension-compression according to three hypotheses of damage accumulation (SK = Serensen-Kogayev, CD = Corten-Dolan, PM = Palmgren-Miner)

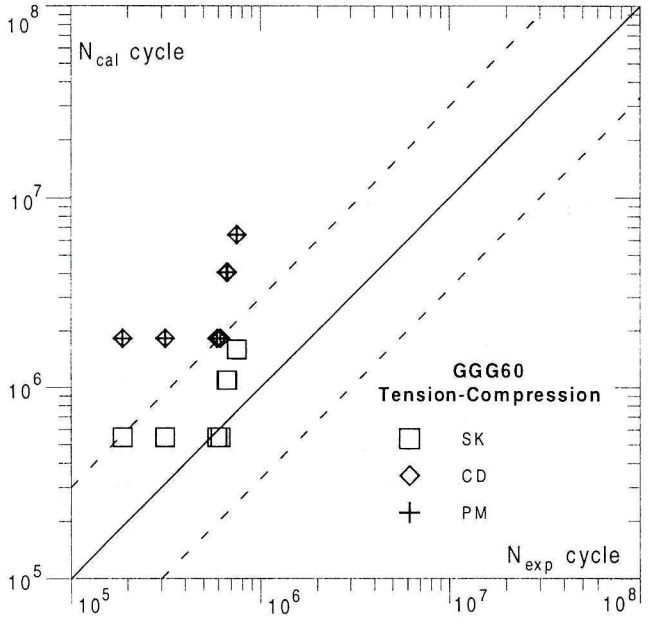

Fig. 7. Comparison of the calculated life N_{cal} and the experimental one N_{exp} for cast iron GGG60 under variable amplitude tension-compression according to three hypotheses of damage accumulation (SK = Serensen-Kogayev, CD = Corten-Dolan, PM = Palmgren-Miner)

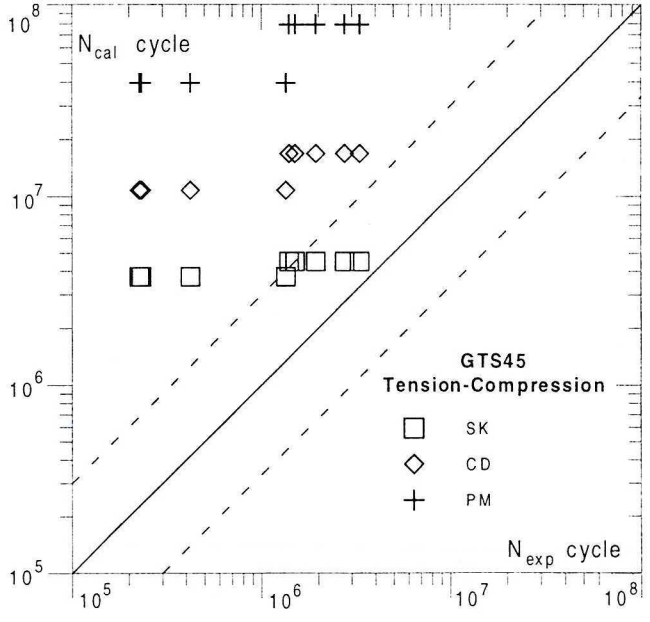

Fig. 8. Comparison of the calculated life N_{cal} and the experimental one N_{exp} for cast iron GTS45 under variable amplitude tension-compression according to three hypotheses of damage accumulation (SK = Serensen-Kogayev, CD = Corten-Dolan, PM = Palmgren-Miner)

Thus, we will use the Serensen-Kogayev hypothesis for further calculations under pure torsion and combined proportional and non-proportional tension-compression with torsion. Figures 9-11 show the calculation results against the experimental data for all the considered cast irons. From the figures it results that most resultes of calculations are included in the scatter band with coefficient 3. Only for cast iron GTS45 greater scatters were obtained, like under uniaxial tension-compression. Under pure tension-compression, the calculated and experimental directions of the critical planes are the same and inclined at the angle 0°. Under pure torsion, these planes aro also the same and their angle is 45°. The calculated directions of the fatigue fracture plane positions for a combination of proportional and non-proportional tension-compression with torsion are included in the range 33–35°, and they agree with the experimental directions (~30°) quite well.

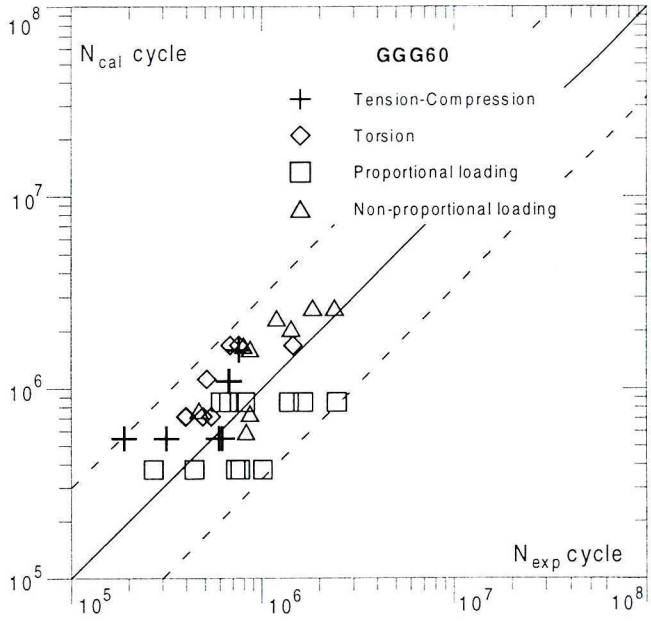

Fig. 9. Comparison of the calculated life N_{cal} and the experimental one N_{exp} for GGG40 cast iron under variable amplitude tension-compression, torsion and proportional and non-proportional tension-compression with torsion according to the Serensen-Kogayev hypothesis

In Fig. 12 one can find the exemplary calculated fatigue lives depending on the assumed angle of the critical plane for GGG40 cast iron. From the above calculations it appears that the maximum damage for the applied criterion as well as the expected fracture angle in the considered case are inclined at 34 degrees to the specimen angle.

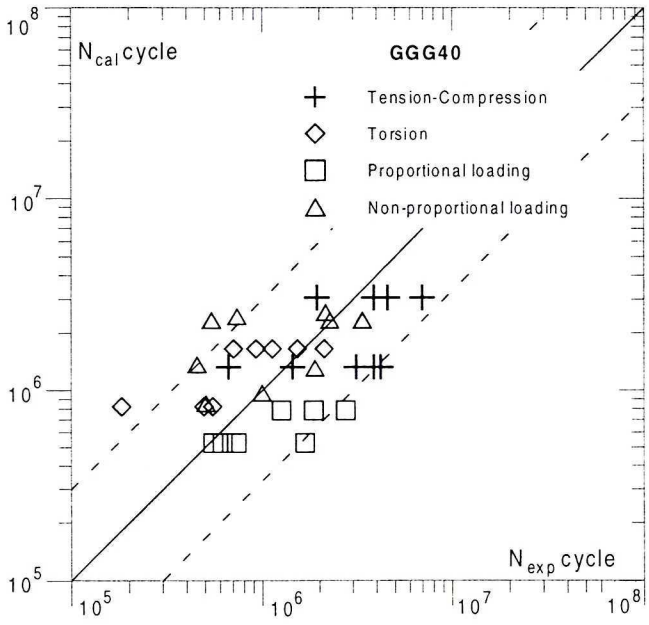

Fig. 10. Comparison of the calculated life N_{cal} and the experimental one N_{exp} for GGG60 cast iron under variable amplitude tension-compression, torsion and proportional and non-proportional tension-compression with torsion according to the Serensen-Kogayev hypothesis

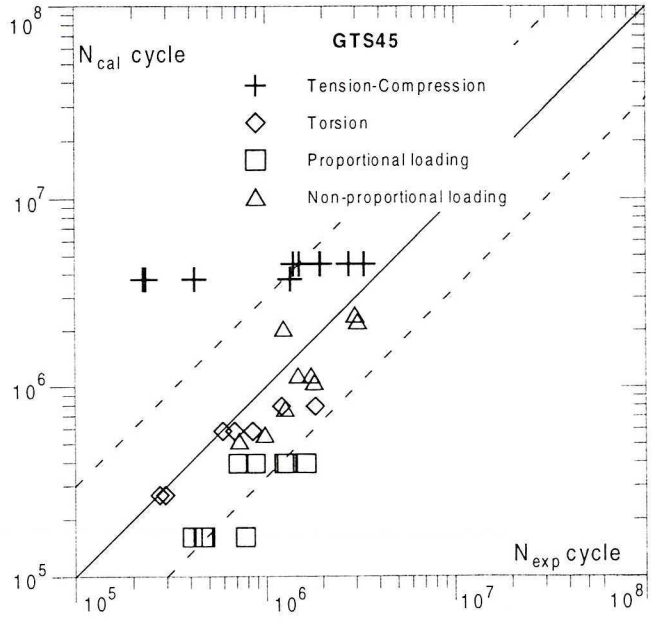

Fig. 11. Comparison of the calculated life N_{cal} and the experimental one N_{exp} for GTS45 cast iron under variable amplitude tension-compression, torsion and proportional and non-proportional tension-compression with torsion according to the Serensen-Kogayev hypothesis

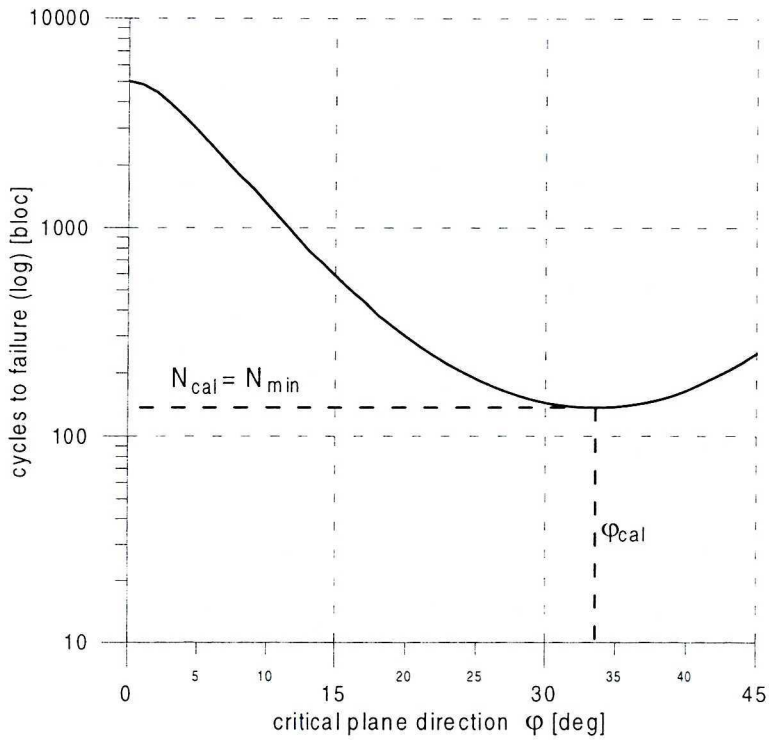

Fig. 12. Results of the fatigue life calculations for particular planes.

5. Conclusions

From the tests under combined variable amplitude tension with torsion for three cyclically hardened cast irons it results that non-proportional loading causes fracture more quickly than proportional loading.

Fatigue damage summation in the tested cast irons seems to be efficient with the use of the Serensen-Kogayev hypothesis. The Palmgren-Miner hypothesis gives unsatisfactory results.

The proposed algorithm for fatigue life estimation, based on the modified criterion of maximum normal stress in the critical plane seems to be useful for analysis of the experimental data obtained for the tested cast irons within the long-life time under proportional and non-proportional variable amplitude loading.

Applying the method of fatigue damage cumulation we obtain the fracture plane direction which agrees with the experimental plane very well.

* * *

The paper realized within the research project 7 T07B 018 18, partly financed by the Polish State Research Committee in 2000–2002.

Manuscript received by Editorial Board, October 24, 2000;
final version, November 29, 2000.

REFERENCES

[1] Łagoda T., Macha E., Będkowski W.: A critical plane approach based on energy concepts: application to biaxial random tension-compression high-cycle fatigue regime. Int. J.Fatigue, vol. 21, 1999, pp.431÷443.

[2] Müller A.: Strength of multiaxial stochastic loaded nodular and malleably cast iron. Fraunhofer-Institut für Betriebsfestigkeit, Bericht Nr. FB-203, Darmstadt 1994, S. 140 (in German).

[3] Neugebauer J.: Fatigue behaviour of cast iron materials under multiaxial loading with different frequencies. Bericht Nr. FB-175, Fraunhofer-Institut für Betriebsfestigkeit (LBF), Darmstadt 1986, S.176 (in German).

[4] Grubisic V., Neugebauer J.: Strength of nodular cast iron under combined static and dynamic multiaxial loading. Bericht Nr. FB-149, Fraunhofer-Institut für Betriebsfestigkeit (LBF), Darmstadt 1979, S.57 (in German).

[5] ASTM E 1049-85 (1997), Standard practices for cycle counting in fatigue analysis, in: Annual Book of ASTM Standards, Vol. 03.01, Philadelphia 1999, pp. 710÷718.

[6] Łagoda T., Macha E.: Estimated and experimental fatigue lives of 30CrNiMo8 steel under in- and out-of-phase combined bending and torsion with variable amplitudes, Fatigue Fract. Engng Mater. Struct., vol. 17, 1994, pp. 1307÷1318.

[7] Corten H.UT., Dolan T.L.: Cumulative fatigue damage. Int. Conf. Metals, The Institution of Mechanical Engineers, London 1956, pp.235÷246.

[8] Miner M.A.: Cumulative damage in fatigue. J. Applied Mechanics, vol. 12, 1945, pp.159÷164.

[9] Palmgren A.: Die Lebensdauer von Kugellagern. VDI-Z, vol. 68, 1924, ss.339÷341.

[10] Serensen S.V., Kogayev V.P., Snajderovic R.M.: Nesuščaja sposobnost i rasčet detalej mašin na pročnost. Izd. 3-e, Mašinostroenie, Moskwa 1975, s.488 (in Russian).

[11] Łagoda T., Macha E.: Estimated and experimental fatigue lives of 30CrNiMo8 steel under in- and out-of-phase combined bending and torsion with variable amplitudes. Fatigue Fract. Engng Mater. Struct., vol. 17, 1994, pp.1307÷1318.

[12] Socie D.F.: Critical plane appraches for multiaxial fatigue damage assessment, Advances in Multiaxial Fatigue. ASTM STP 1191, D.L. McDowel and R.Ellis, Eds., American Society for Testing and Materials, Philadelphia, 1993, pp.7÷36.

[13] Wang C.H., Brown M.W.: A path-independent parameter for fatigue under proportional and non-proportional loading, Fatigue Fract. Engng Mater. Struct., vol 16, 1993, pp.1285÷1298.

[14] Morel F.: A mesoscopic approach to describe the high cycle fatigue behaviour of metals submitted to multiaxial loading. Scientific Papers of the Institute of Materials Science and Applied Mechanics of the Wroclaw University of Technology No 60, Conferences No 8, Wrocław 1998, pp.12÷54.

[15] Papadopoulos I.V.: A new criterion of fatigue strength for out-of-phase bending and torsion of hard metals. Int. J. Fatigue, vol 16, 1994, pp.377÷384.

[16] Lease K.B., Stephens R.I.: Fatigue of A356-T6 cast aluminum alloy under variable amplitude loading. Proc. Fourth Int. Conf. on Fatigue and Fatigue Thresholds, Fatigue '90, H.Kitagawa and T.Tanaka, Eds., Materials and Component Engng Publications 1990, I, pp.493÷498.

[17] Perov S.N., Ogarevic V.V., Stephens R.I.: Application and verification of fatigue life calculation methods for AZ91E-T6 cast magnesium alloy under variable amplitude loading. J. Engng Mater. Technol. ASME, vol.115, 1993, pp.385÷390.

[18] Smith K.N., Watson P., Topper T.H.: A stress-strain function for the fatigue of metals. Journal of Materials, Vol.5, 1970, pp.767÷776.

[19] Fatemi A., Socie D.F.: A critical plane approach to multiaxial fatigue damage including out-of-phase loading. Fatigue Fract. Engng. Mater. Struct., vol.11, 1988, pp.149÷165.

Trwałość zmęczeniowa żeliwa GGG40, GGG60 i GTS45 przy kombinacji zmienno-amplitudowego rozciągania ze skręcaniem

Streszczenie

W pracy analizowane są wyniki badań zmęczeniowych próbek z trzech rodzajów żeliwa w warunkach proporcjonalnego i nieproporcjonalnego zmienno-amplitudowego rozciągania ze skręcaniem. Dane eksperymentalne z zakresu długotrwałej wytrzymałości zmęczeniowej są porównywane z obliczonymi według algorytmu wyznaczania trwałości zmęczeniowej przy użyciu zmodyfikowanego kryterium maksymalnego naprężenia normalnego w płaszczyźnie krytycznej. Nieprzydatna dla badanego żeliwa i warunków obciążenia okazała się w tym algorytmie liniowa hipoteza kumulacji uszkodzeń Palmgrena–Minera. Natomiast zadawalające wyniki uzyskano stosując nieliniową hipotezę Serensena–Kogayeva. Stosując metodę kumulacji uszkodzeń zmęczeniowych uzyskan0 bardzo dobra zgodność obliczeniowych płaszczyzn krytycznych z eksperymentalnymi.